Desalination and Water Treatment
www.deswater.com
doi: 10.5004/dwt.2020.26279

206 (2020) 177–188
December

Studies on properties and adsorption ability of bilayer chitosan/PVA/PVDF electrospun nanofibrous

Nur Areisman Bin Mohd Salleh[a,*], Amalina M. Afifi[a,*], Fathiah Binti Mohamed Zuki[b], Norazilawati Muhamad Sarih[c], Katayoon Kalantari[d], E. Niza Mohamad[a]

[a]*Department of Mechanical Engineering, Faculty of Engineering, University of Malaya, Kuala Lumpur, Malaysia, emails: nurariesmansalleh@siswa.edu.my (N.A.B.M. Salleh), amalina@um.edu.my (A.M. Afifi)*
[b]*Department of Chemical Engineering, Faculty of Engineering, University of Malaya, Kuala Lumpur, Malaysia*
[c]*Department of Chemistry, Faculty of Science, University of Malaya, Kuala Lumpur, Malaysia*
[d]*Chemical Engineering, Northeastern University, Boston, MA, USA*

Received 15 December 2019; Accepted 21 June 2020

ABSTRACT

In this new era of nanofiber industry, the practice of using electrospun nanofiber membrane technology for wastewater treatment is increasingly becoming common. However, there are lacks of studies in the aspect of mechanical properties, especially strength. Therefore, the bilayer nanofiber membranes were introduced in order to improve the strength of the membrane. A chitosan solution (7 wt.% chitosan in concentrated acetic acid) and polyvinyl alcohol (PVA) solution (8 wt.% PVA in distilled water) was blended for 24 h and the solution mixture was electrospun according to the optimized parameters to get a fine nanofiber. Then, the polyvinylidene fluoride (PVDF) solution was electrospun on top of chitosan/PVA nanofiber to make a bilayer nanofiber membrane. Crosslinking process were done in order to improve the wettability and mechanical properties. The chitosan/PVA-PVDF bilayer nanofiber was identified with field emission scanning electron microscopy, Fourier transform infrared, wettability, swelling, tensile, and adsorption tests. The nanofiber membrane was stable in the acidic, base, and neutral mediums for 20 d, and the tensile strength increased from 0.17 to 0.65 MPa. Additionally, the adsorption efficiency of the bilayer nanofiber membrane was investigated over Cr(VI) and Fe(III) ions using Langmuir and Freundlich isotherm. Kinetic parameters were evaluated using the first-order and pseudo-second-order models. Kinetic study showed that the adsorption rate was high at a lower concentration of the metal ion. Thus, the bilayer nanofiber membrane is highly potential to increase the mechanical properties of the nanofiber membrane while maintaining the adsorption efficiency.

Keywords: Chitosan; Polyvinyl alcohol; Polyvinylidene fluoride; Electrospun nanofibrous; Adsorption

1. Introduction

Water is a salient element on earth. Most of the life form needs water in order to ensure their survival. Seventy-one percent of the earth is covered by water and only 2.5% of them can be considered as freshwater [1]. In addition, water resources are affected by pollution and a gradual increase in the population. Some regions in the world already considered water as a crucial commodity and in a recent finding, 80% of the world population is on the cautious state on high levels of threat to water security [2].

Nowadays, heavy metal pollution in the groundwater has become a global threat due to its environmental issues,

* Corresponding authors.

profusion in number and persistence [3–5]. A lofty concentration of heavy metals could trigger harmful biochemical reactions and affect human health such as inhibition of enzymes, genetic damage, and hypertension [6]. There are studies that prove the relationship between water quality and transience from cardiovascular and other ceaseless diseases. Various types of cancer have also been linked to concentration of particular heavy metals in water supplies [7].

There are a few methods that have been used in water treatment such as coagulation, adsorption, dialysis, membrane process, foam flotation, osmosis, and biological methods [8]. However, there are limiting factors such as cost and efficiency which prevent from these methods being fully utilized. Lately, there are proven studies that shows electrospun nanofibers membranes (ENMs) for water treatment applications due to their unique and good properties such as high surface area-to-volume ratio, large porosity, and good water permeability [9] which make them as promising materials for adsorption of heavy metals [10]. Numerous studies have shown the efficiency of nanofiber in treating wastewater by adsorption of heavy metal ion. For example, fabrication of nanofibers using sodium alginate and poly(vinyl alcohol) tested for the removal of Cd^{2+} shows high cadmium uptake [11]. In another study, chitosan/polyvinyl alcohol/TiO_2 nanofiber composite have been fabricated and exhibit good dye removal rate [12]. In spite of many favorable properties, electrospun nanofiber membranes also exhibit difficulties such as insufficient hydrophilicity, high swelling rate, low mechanical strength, membrane fouling, gel layer formation, and blockage of solute by adsorption process on pore walls [13]. On top of that, electrospun membranes from bio-based polymeric materials are not yet commercially available.

Chitosan, a prominent material that has been used for electrospun nanofiber membrane is made up from crystalline microfibrils of crustacean such as crabs and prawns. It is biodegradable and has the properties to fix a wide range of heavy metals and radio-nuclides [14]. Nevertheless, chitosan exhibits unstable mechanical properties, pH-sensitive, and susceptible to swelling [15]. In order to improve the spin-ability, another polymer such as polyvinyl alcohol (PVA) is blended with the chitosan for electrospinning process [16]. PVA also reduces the crystallinity of the chitosan structure to some extent [13].

Generally, chitosan electrospun nanofibers exhibit good adsorption properties but weak in mechanical properties [17]. It is easy to dissolve in the moisture environment, lost its integrity, and difficult to be removed from the collector [18]. In order to overcome the mechanical and physical properties issues, polyvinylidene fluoride (PVDF) has been introduced as a nanofiber bilayer with chitosan/PVA nanofiber. PVDF exhibits good mechanical property, high chemical resistance, and good thermal stability [19]. In the present study, a bilayer nanofiber membrane was fabricated using an electrospinning method and run for characterization and application tests. In contrast to previous studies that only used a single membrane, our fabricated membrane was composed of two different nanofiber membranes which were assembled in a layered form. The primary goal of this study is to investigate the efficiency a wastewater treatment membrane of the bilayer membrane: chitosan/PVA nanofiber membrane which is hydrophilic and PVDF nanofiber membrane which is hydrophobic and to determine the function of PVDF layer as a support frame to achieve good mechanical and physical properties for the bilayer nanofiber membrane.

2. Materials and methods

Chitosan (M_w = 8.96 × 10^5 g/mol, degree of deacetylation = 40%, and acetone were purchased from SE Chemical Co., Ltd., (Tokyo, Japan) and System (Selangor, Malaysia), respectively. PVA (M_w = 146,000–186,000 g/mol, DDA = 99%), PVDF (M_w = 534,000), acetic acid, $FeCl_3 \cdot 6H_2O$, and $K_2Cr_2O_7$ were purchased from Sigma-Aldrich (United States) while NaOH and DMF were obtained from R&M Chemicals (United Kingdom).

2.1. Hydrolysis of chitosan

The DDA of chitosan exhibits the transformation of N-acetyl-D-glucosamine to D-glucosamine [20]. The molecular weight and DDA of supplied chitosan are not suitable for the electrospinning process. Low molecular weight chitosan is easier to align effectively in the electromagnetic field of the electrospinning process thus improve the spin-ability. In addition, higher DDA is favorable in the solubility of chitosan [21]. Thus, the hydrolysis process leads to an increase in the DDA of chitosan and simultaneously decreases the molecular weight of chitosan [22]. In this study, 40 g of NaOH was mixed with 80 g of distilled water and later, 2.5 wt.% of chitosan was added to the mixture. The solution was stirred at 90°C for 24 h. Next, the solution was filtered using a vacuum flask and cleansed using distilled water. Finally, the filtered chitosan has placed an oven at 60°C for 4 h to completely dry.

2.2. Preparation of chitosan/PVA and PVDF solutions

7.0 wt.% of chitosan was completely dissolved in 10% acetic acid. Chitosan solution was mixed with 8.0 wt.% PVA solution in a 50:50 weight ratios. Previous study showed that this ratio exhibited defects free morphology under the same condition [13]. For the preparation of PVDF solution, 1.5 g of PVDF were mixed with 7 mL of DMF at 70°C for 24 h, later 3 mL of acetone were added into the solution and stirred at room temperature for 24 h.

2.3. Electrospinning

First, the electrospinning of PVDF as a supportive scaffold was performed by using 22G blunt stainless steel needle (0.7 mm outer diameter and 0.4 mm inner diameter, 15 cm tip-to-collector distance, 20 kV applied voltage, 500 rpm for collector drum roll, and 30–200 mm scanning position (the horizontal movement of syringe platform) with speed 100 mm/min. Then, the chitosan/PVA were electrospun directly onto the electrospun PVDF membrane with the same condition, except for the applied voltage which ranged between 13 and 17 kV. Finally, the obtained samples were

placed in the desiccator with glutaraldehyde vapor for 24 h to produce cross-linked sample.

2.4. Characterization

In order to determine the bonding behavior between chitosan/PVA and PVDF, and glutaraldehyde, Fourier transform infrared (FTIR) spectroscopy (Nicolet iS10 FTIR spectrometer from Thermo Scientific, United States) was applied with spectral range between 400 and 4,000 wavenumbers with a resolution of 4 cm^{-1}. The surface and morphologies of the membrane were observed using field emission scanning electron microscopy (SEM, Hitachi SU5000 VPFESEM, Tokyo, Japan) and samples were coated with platinum to avoid charging which will affect the images. The analysis of fiber diameter size was done using ImageJ software. The wettability of the samples was tested by using contact angle analysis (Dataphysic Instrument OCA 15EC, Germany). Samples were placed on a platform and sessile drop methods with 5 μL droplet condition were carried out. The mechanical properties of the sample were tested in dry condition using a universal tensile testing machine (Shimadzu AGS-X series, Kyoto, Japan) equipped with 50-N load cell at room temperature. The test was done with a constant elongation velocity of 5 mm/min. The durability of the bilayer nanofiber was tested with swelling test. Three different mediums, base (pH = 10), acidic (pH = 3), and neutral (pH = 7) were used in this research. The samples were weighted and then immersed in the mediums for 20 d. After that, the sample were dried and weighted. Swelling ratio was calculated by using the following formula [23]:

$$S_w = \frac{W_s - W_d}{W_d} \times 100 \quad (1)$$

where W_s and W_d indicate the mass before and after immersion in water, respectively.

2.5. Adsorption study

The adsorption property of chitosan/PVA-PVDF bilayer nanofiber was assessed with metal ion adsorption behavior. The membrane was tested with Cr(VI) and Fe(III). 0.2 g of membrane samples were stirred with 30 mL of potassium(VI) dichromate and iron(III) chloride solutions, using a lab shaker to ensure the maximum contact of the membrane surface with the metal ions present in the solution. Initially, each of the heavy metal ions concentration was varied and at a certain time interval, the concentration was calculated by using a flame atomic absorption spectrometer (Analyst 400, Perkin Elmer, United States). The adsorption of heavy metals ions by the nanofiber was evaluated with the following formula [24]:

$$q_t = \frac{C_0 - C_t}{m} V \quad (2)$$

where C_0 and C_t are the concentration of heavy metal ion (mg/L) at initial and equilibrium respectively, V is the volume of the solution (L), and m is the mass of the sample (g).

3. Results and discussion

3.1. FTIR analysis

To verify the process of bindings, analysis on FTIR spectra of PVA, chitosan-PVA and chitosan-PVA (cross-linked) were done as shown in Fig. 1. The absorption peak at 1,261 cm^{-1} in PVA graph indicated the O–H band and in chitosan/PVA graph, was shifted to 1,282 cm^{-1} with low frequency [25]. The adsorption peak at 3,322 cm^{-1} indicated the primary amine in the chitosan/PVA. The absorption peak at 1,328 cm^{-1} represents the $–CH_2$ bonded with –OH group, which can be found in the spectra of PVA and chitosan-PVA [26]. There are common peaks in the range of 1,000–1,200 cm^{-1} which is the characteristic peaks of C–O vibration of chitosan and PVA molecule [27]. Peak at 1,412 cm^{-1} were the results of wagging vibration of C–H in PVA and chitosan/PVA [28]. The peak at 1,234 cm^{-1} indicated C–O–C formed through the crosslinking process, between OH of common PVA structure and –C– of glutaraldehyde molecule. The broad peak 3,319 cm^{-1} is due to the stretching vibration of OH group, which is characteristic peak for both PVA and chitosan/PVA [29]. Other characteristic peaks such as 1,404; and 2,908 cm^{-1} also explain the presence of PVA that extend over Chitosan-PVA. These results show that the chitosan was successfully blended with PVA and form a nanofiber.

Fig. 2 shows the FTIR peak for PVDF side of the bilayer membrane. The peak at 836 and 880 cm^{-1} indicated C–C–C asymmetrical stretching vibration of PVDF while peak at 1,174 cm^{-1} represents C–C band of PVDF and peak at 1,404 cm^{-1} is due to the wagging vibration of CH_2 [30]. The results show no bonding between the PVDF and chitosan/PVA nanofiber as the peaks only represent the PVDF characteristic.

3.2. Field emission scanning electron microscopy

By using Field emission scanning electron microscopy (FESEM), the morphology of the nanofiber bilayer was also studied. Fig. 3 shows the FESEM micrographs of the nanofiber bilayer. The mean diameter for PVDF nanofiber is 394.08 nm. The image shows fine fiber with a small amount of beads formation. The chitosan/PVA solution were successfully electrospun into nanofiber with a mean diameter of 116.5 and 101.18 nm for the crosslinked nanofiber.

In order to confirm the presence of elements, the nanofiber bilayer was analyzed by energy dispersive X-ray spectrometry (EDS). In Fig. 4, the spectra show the peaks of O, C, and F which represents the main element in PVDF and chitosan/PVA nanofiber composite.

3.3. Contact angle

Contact angle is the prominent method to study the wettability of the nanofiber membrane. This method provides a direct evaluation of surface wettability by allowing the formation of geometric measurement or angle at the intersection of different phases such as gas, liquid, and solid. Higher contact angle (>90°) represents a hydrophobic surface while a lower contact angle (<90°) represents a hydrophilic surface. For better adhesion and higher surface

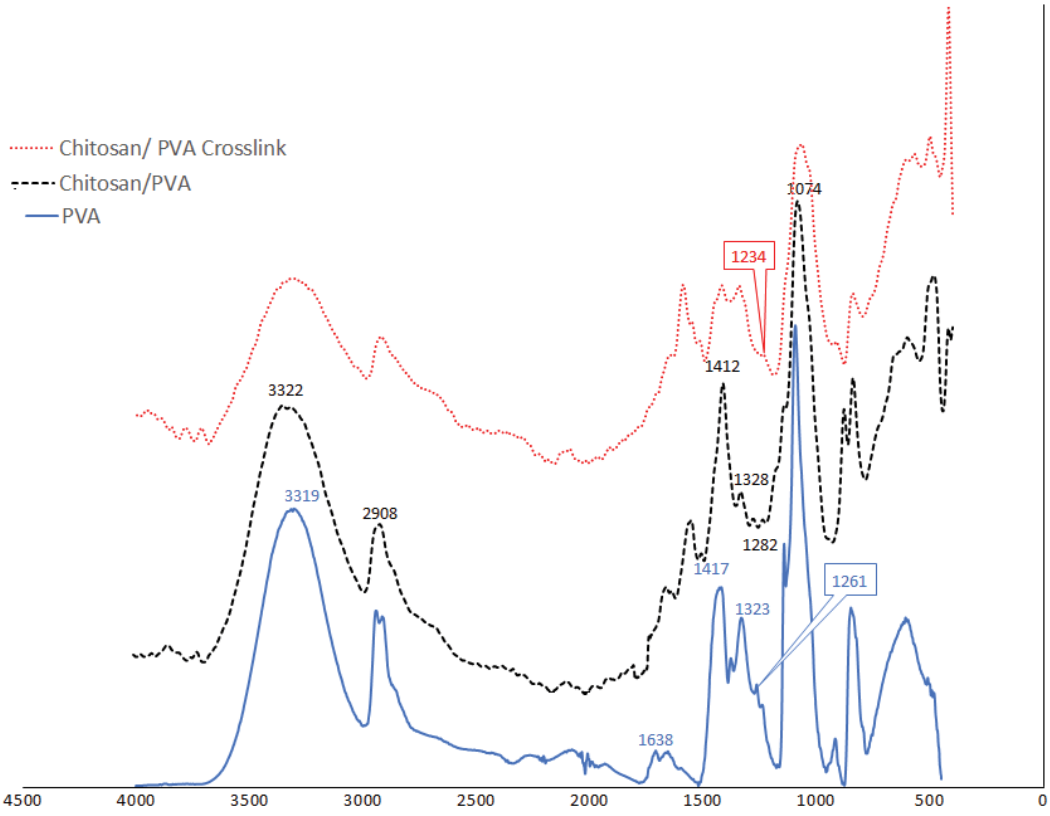

Fig. 1. FTIR spectra of chitosan/PVA nanofiber.

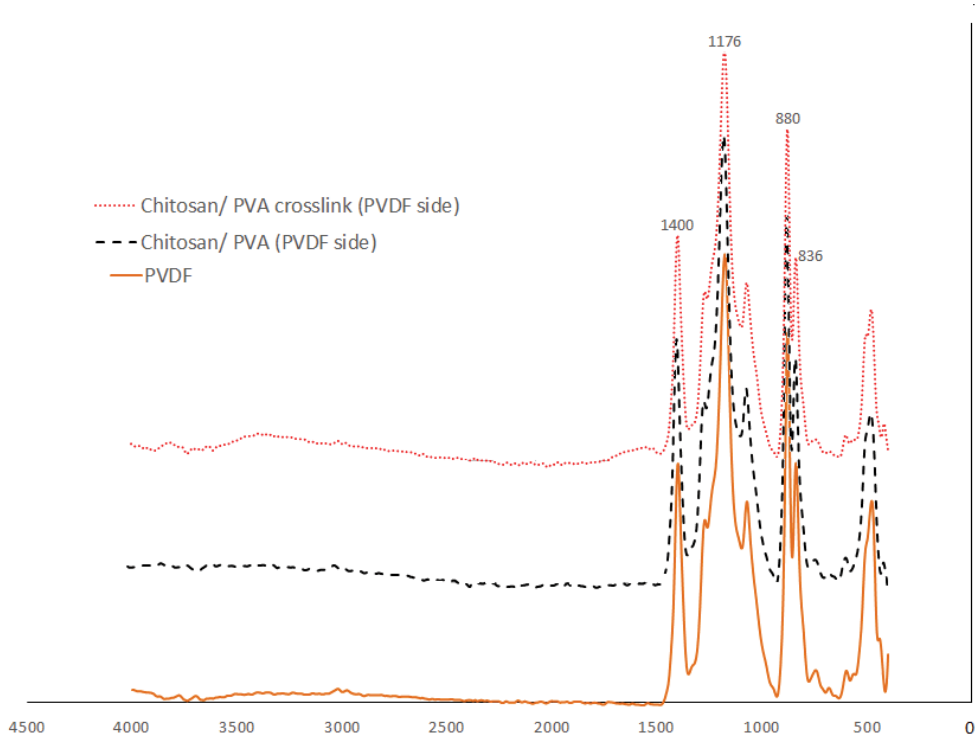

Fig. 2. FTIR spectra of PVDF.

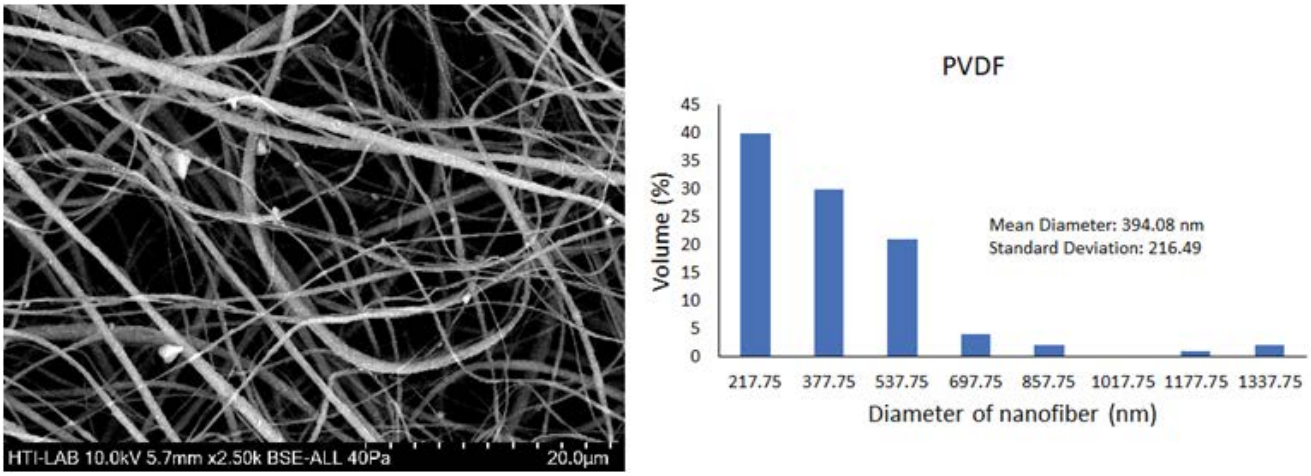

(a)

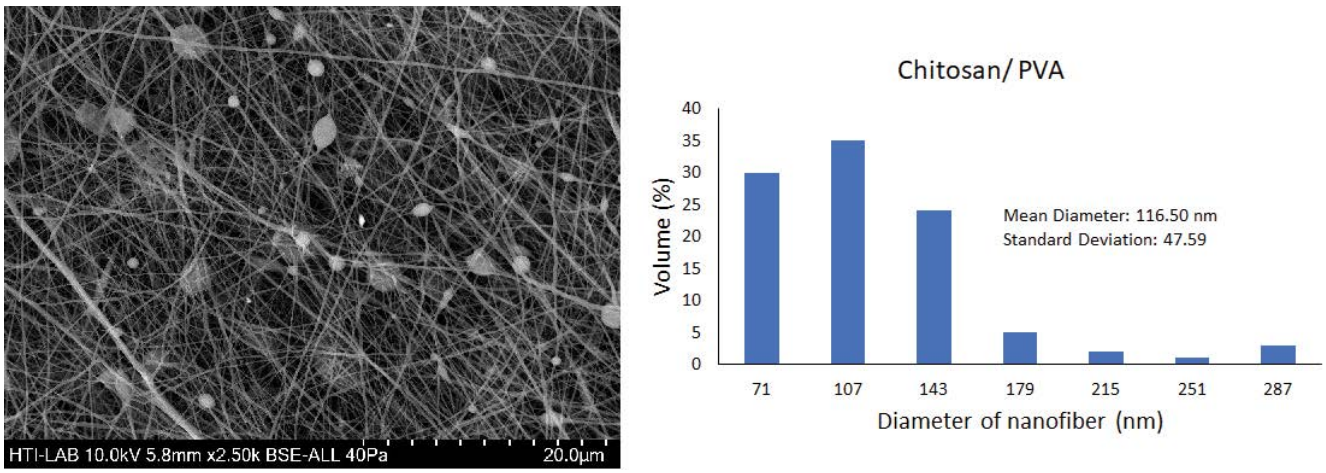

(b)

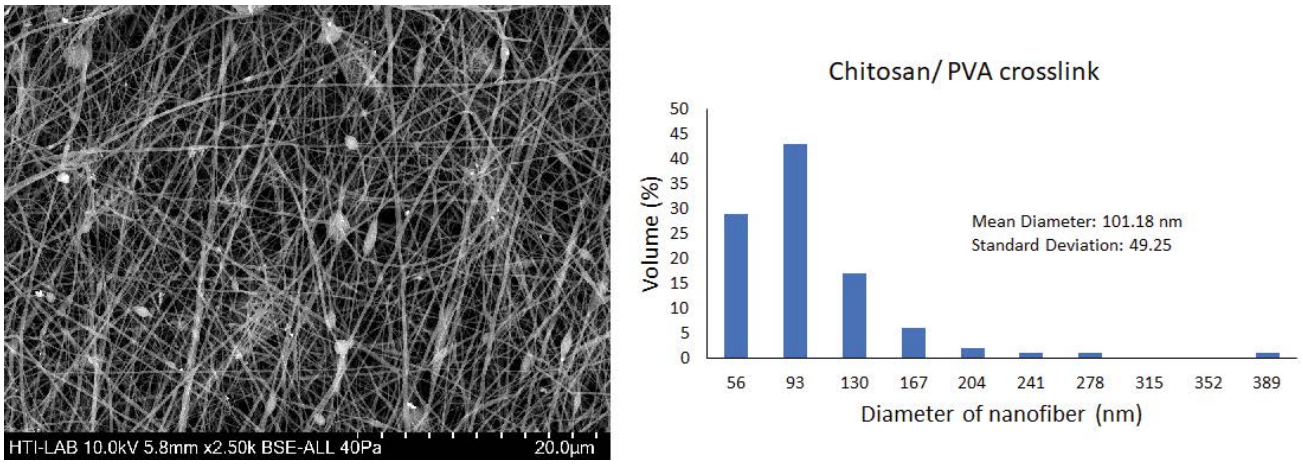

(c)

Fig. 3. FESEM of nanofiber composite (a) PVDF, (b) chitosan/PVA, and (c) chitosan/PVA crosslink.

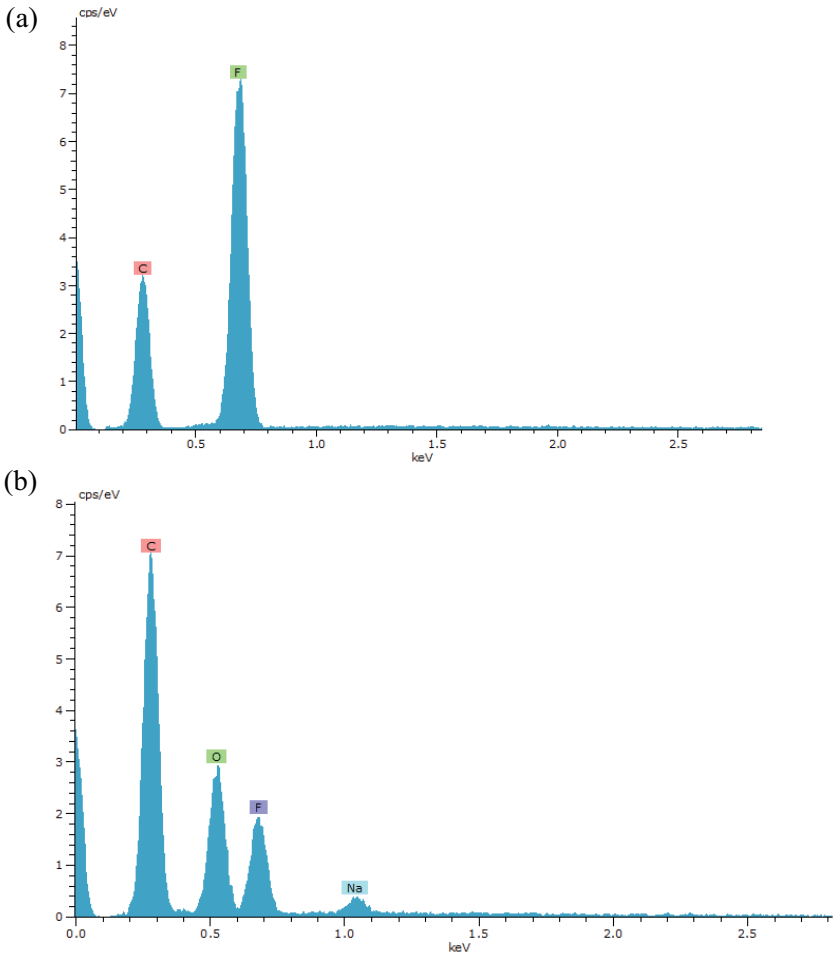

Fig. 4. EDS of (a) PVDF and (b) chitosan/PVA nanofiber composite.

energy, a lower contact angle is preferred as the hydrophilic surface represent those properties [31]. In Fig. 5, the degree of contact angle of the nanofiber membrane can be categorized into hydrophilic and hydrophobic.

Nanofiber chitosan/PVA-PVDF (chitosan/PVA side) has the lowest value, 35.45° while nanofiber chitosan/PVA crosslink-PVDF (chitosan/ PVA cross-linked side) has increased to 52.93°. This is due to the presence of a crosslink agent, glutaraldehyde which prevents the water from spreading and penetrate the nanofiber [32]. For the PVDF side, both samples exhibited hydrophobic properties which lead to a rigid membrane and act as a supporting frame for the chitosan/PVA membrane.

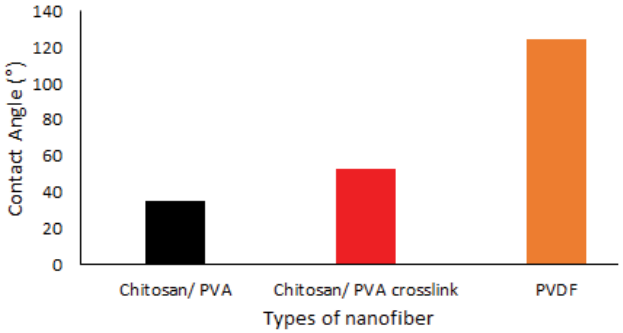

Fig. 5. Contact angle of the nanofiber composite.

3.4. Swelling test

In this test, all nanofiber samples were immersed for 20 d in three different mediums; acidic, neutral, and base to evaluate the integrity of the membrane. In Fig. 6, most of the nanofibers exhibit shrinkage and weight loss due to the dissolution of PVA in the medium. However, the sample for chitosan/PVA crosslink-PVDF shows considerable stability with a slight change in weight and swelling ratio. Several factors can be related to this phenomenon such as the PVDF homophobic properties, insolubility of chitosan fraction [33], hydrogen bonding along with chitosan, and PVA [34] and the crosslinking effect in chitosan/PVA composite [35].

3.5. Tensile test

Fig. 7 shows the stress–strain graph of chitosan/PVA nanofiber membrane and chitosan/PVA-PVDF bilayer nanofiber membrane. The maximum tensile stress increases from 0.17 to 0.65 MPa. The interaction between PVDF and

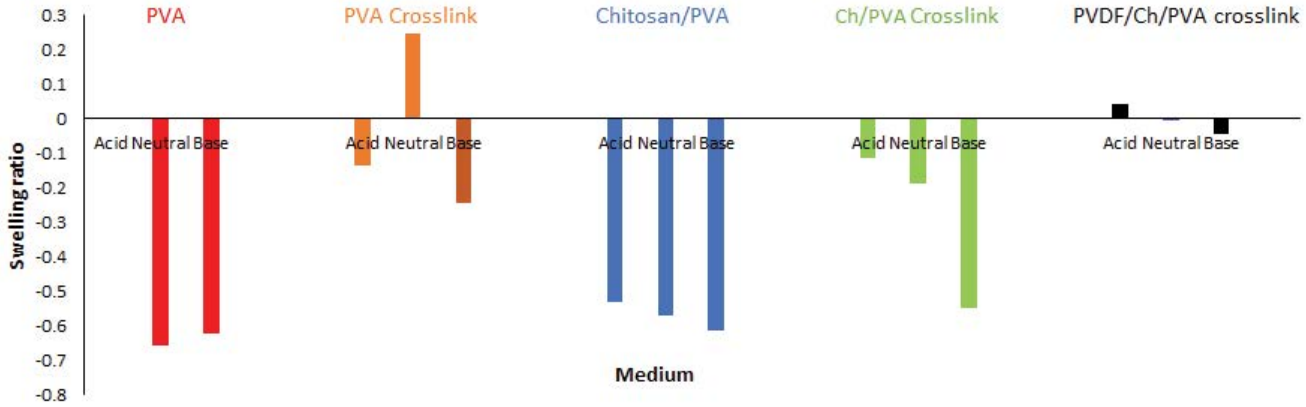

Fig. 6. Swelling ratio of the nanofiber composites.

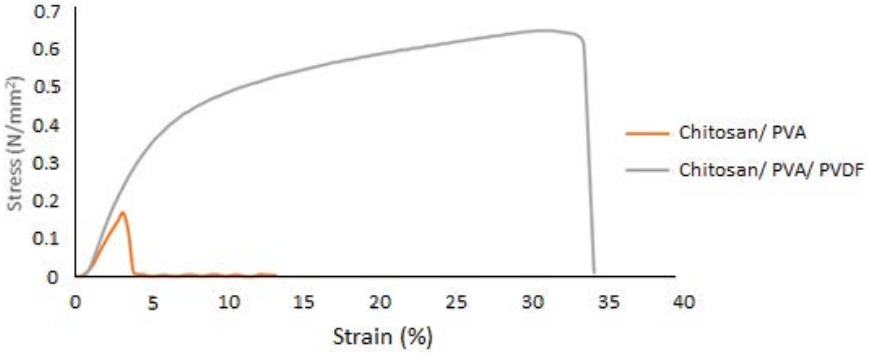

Fig. 7. Stress vs. strain graph.

chitosan/PVA nanofiber layer prevents an instant failure after the applied stress surpasses the ultimate tensile strength of the chitosan/PVA membrane and the bilayer exhibits good toughness due to the presence of PVDF layer which is known for its good mechanical resistance properties [36]. In the bilayer nanofiber membrane, strain hardening made the fiber aligned to the stress direction and localized necking. It also exhibits multiple microfracture events, different from the traditional fractures [37]. Moreover, the increase in the tensile stress is due to the strong physical interaction between the two layers which eases the stress transfer at the interface and improves the stiffness of the nanofiber membranes [17]. It is also proven that PVDF layer also acts as a "hard" coating, masking the defect in the chitosan/PVA nanofiber layer with good adhesion properties [38].

3.6. Adsorption kinetics

The relationship between heavy metal ions with the surface of the adsorbent can be explained by its adsorption kinetics. In this experiment, two most common diffusion models were used which are Lagergren-first-order and pseudo-second-order. The linear forms of these models are shown below [39,40], respectively.

$$\log\left(q_e - q_t\right) = \log q_e - \frac{k_1 t}{2.303} \tag{3}$$

$$\frac{t}{q_t} = \frac{1}{k_2 q_e^2} + \frac{t}{q_e} \tag{4}$$

where q_e and q_t represent the concentration (mL/g) of heavy metal at equilibrium and at contact time t (min) respectively. k_1 (min^{-1}) and k_2 (g/mmol min) are the rate constant for Lagergren-first-order and pseudo-second-order model, respectively. The value of rate constant was evaluated to study the adsorption process. Figs. 8 and 9 indicate the linear plot of Lagergren-first-order and pseudo-second-order for both heavy metal ion adsorptions. Table 1 summarizes the whole data of kinetic parameters. According to Figs. 8 and 9, adsorption of Cr(VI) can be explained by using pseudo-second-order model which indicates the adsorption process is chemical adsorption. The process was affected by sharing or exchange of electrons between the metal ion and the nanofiber [41] while for Fe(III), the adsorption obeys the Lagergren-first-order model which indicated the main process of adsorption was physisorption.

3.7. Adsorption isotherm

In order to study the relationship between adsorbate and adsorbent, adsorption isotherm was used in this study. Specifically, in this study, Langmuir and Freundlich isotherm were used. The equation for Langmuir isotherm is shown as below [42]:

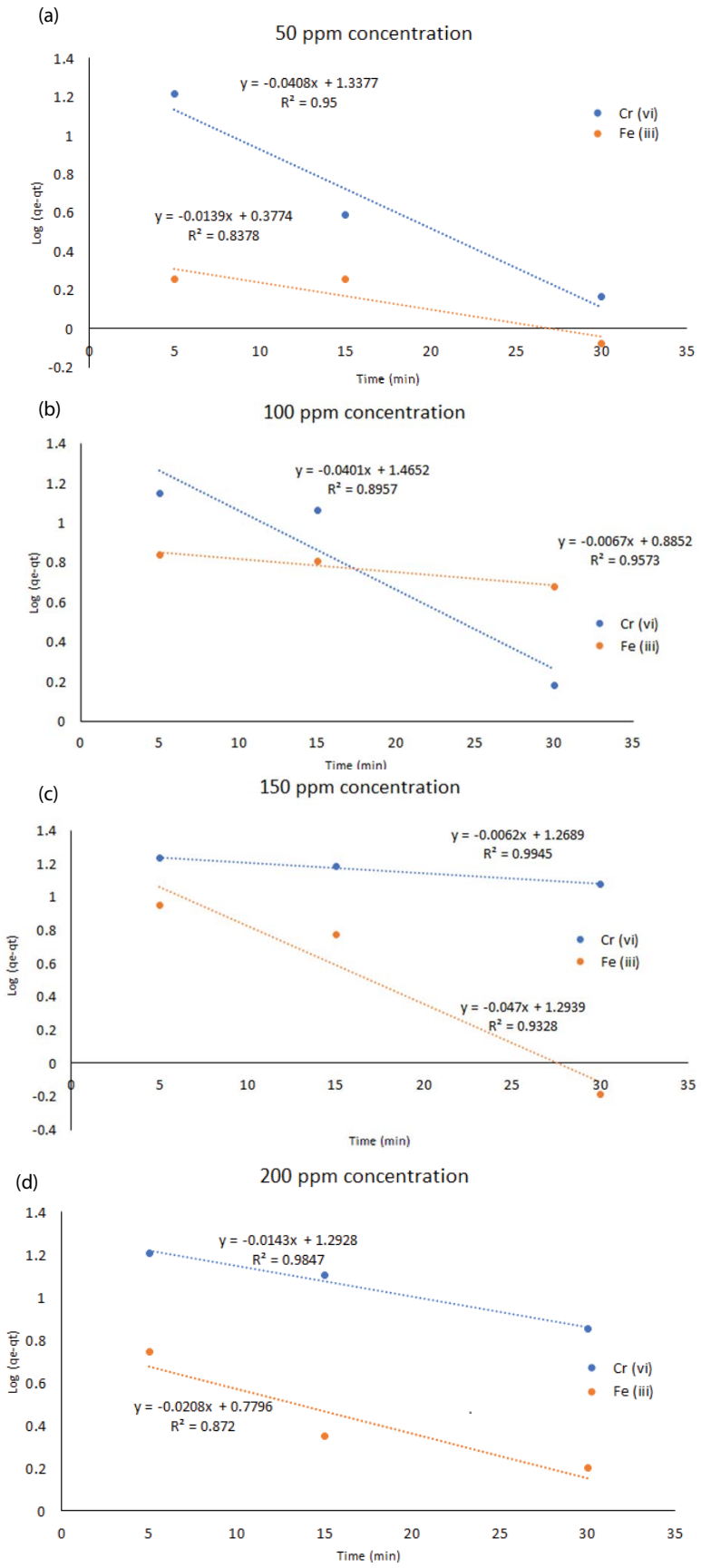

Fig. 8. Lagergren-first-pseudo-order model of Cr(VI) and Fe(III) (a) 50 ppm, (b) 100 ppm, (c) 150 ppm, and (d) 200 ppm concentration.

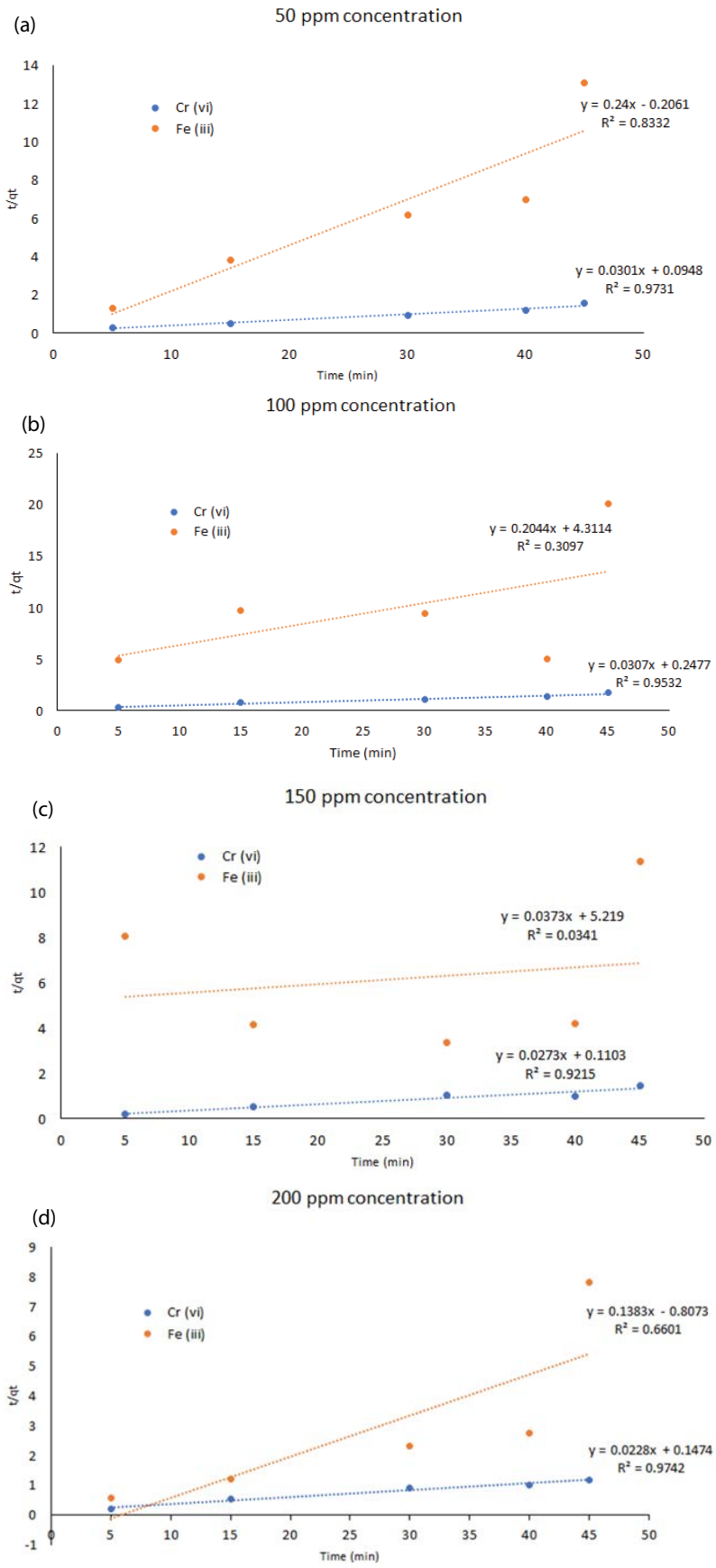

Fig. 9. Second-pseudo-order model of Cr(VI) and Fe(III) (a) 50 ppm, (b) 100 ppm, (c) 150 ppm, and (d) 200 ppm concentration.

Table 1
Parameters of kinetic models

Heavy metal ions	Concentration (ppm)	$q_{e,exp}$ (mmol/g)	Lagergren-first-order constant			Pseudo-second-order constant		
			$q_{e,calc}$	k_1	R^2	$q_{e,calc}$	k_2	R^2
Cr^{6+}	50	33.09	21.76	0.093	0.95	31.94	0.019	0.9731
	100	29.02	29.18	0.092	0.8957	32.57	0.0038	0.9532
	150	40.28	18.57	0.0142	0.9945	36.6	0.0067	0.9215
	200	40.42	19.62	0.032	0.9847	40.48	0.0076	0.9742
Fe^{3+}	50	5.71	2.38	0.00603	0.8378	4.16	–0.148	0.8332
	100	7.93	7.67	0.0029	0.9573	4.89	0.00368	0.3097
	150	9.52	19.62	0.0204	0.9328	26.81	0.00211	0.0341
	200	14.56	6.02	0.00903	0.872	7.23	–0.0058	0.6601

$$= \frac{q_m k_a C_e}{1 + k_a C_e} \tag{5}$$

Thus, the linear form of Langmuir equation as follows:

$$\frac{C_e}{q_e} = \frac{C_e}{q_m} + \frac{1}{K_L q_m} \tag{6}$$

where q_e (mL/g) is the amount of heavy metal ions adsorbed per unit mass of adsorbent, C_e (mmol/L) is the concentration of the leftover heavy metals ions in the solution at equilibrium, q_m is the maximum concentration of heavy metals adsorbed per unit mass of adsorbent and K_L (L/mmol) is the constant of the binding sites. For Freundlich isotherm, the linear form is as follows [42]:

$$\ln q_e = \ln K_F + \frac{1}{n} \ln C_e \tag{7}$$

where q_e represents the amount of metal ion adsorbed per unit of adsorbent at equilibrium (mg g^{-1}) while K_F and n are

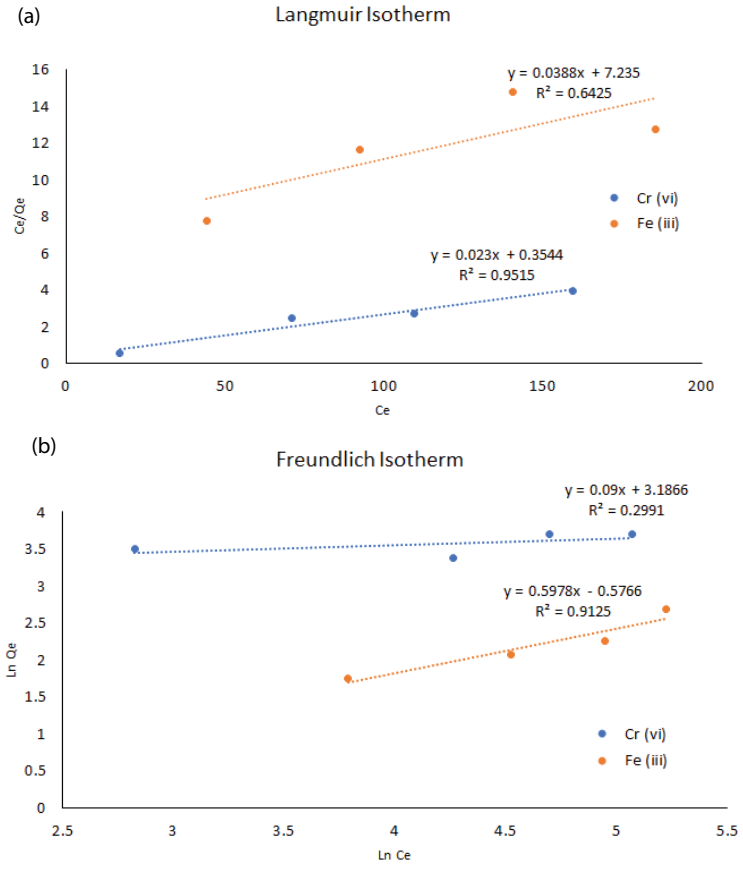

Fig. 10. (a) Langmuir and (b) Freundlich isotherm for Cr(VI) and Fe(III).

Table 2
Parameters of adsorption isotherm

Heavy metal ions	Langmuir Isotherm				Freundlich Isotherm		
	q_m	K_L	R_L	R^2	K_F	n	R^2
Cr^{6+}	43.47	0.0649	0.261	0.9515	24.20	11.11	0.2991
Fe^{3+}	25.77	0.00536	0.878	0.6425	0.56	1.67	0.9125

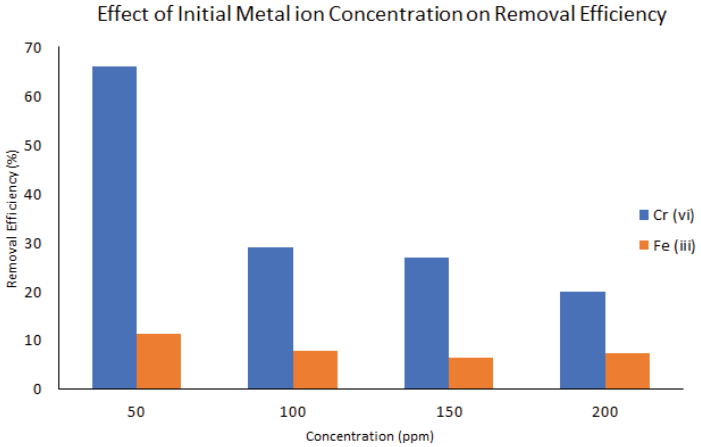

Fig. 11. Removal efficiency for Cr(VI) and Fe(III).

Freundlich constant that shows the capacity of the adsorbent (mg g^{-1}) and the intensity of the adsorption mechanisms, respectively.

Fig. 10 and Table 2 show the Langmuir isotherm and Freundlich isotherm for Cr(VI) and Fe(III) adsorption on nanofiber bilayer and data of adsorption isotherm. The results confirmed the process of adsorption of Cr(VI) is due to the monolayer adsorption [43] onto the homogenous nanofiber membrane and the value of R_L is between 0 and 1, indicates a favorable adsorption process [44]. Meanwhile, for Fe(III) the data obey the Freundlich isotherm which signifies heterogeneous surface and the value of $n > 1$ shows that the process of adsorption is by physical adsorption [45].

Fig. 11 shows the relationship between initial concentration and removal efficiency of the nanofibrous membrane. Both metal ions show significantly decreasing removal efficiency with increasing initial concentration. This is due to the adsorption sites of the nanofibrous membrane decrease at high concentration of heavy metal ion [46]. In addition, the removal efficiency of Cr(VI) were better than Fe(III). This phenomenon is due to the size of the ionic radius of the metal ion. The ionic radius of Fe(III) and Cr(VI) are 69 and 58 pm, respectively. Higher ionic radius leads to lower net charge of the metal ion, thus, metal ion with lower ionic radius has high availability to adsorb other metal ion and leads to higher removal efficiency.

4. Conclusion

Based on the results obtained, the chitosan/PVA-PVDF bilayer nanofibrous membrane was successfully produced via electrospinning process. The bilayer membrane was characterized with FTIR, FESEM, swelling test, contact angle, and tensile test, while the efficiency was studied using adsorption kinetics and adsorption isotherm with Cr(VI) and Fe(III) metal ions. The stability of the bilayer membrane is proven by exhibiting better tensile properties compared to the monolayer nanofiber membrane. For adsorption isotherm, Cr(VI) obeys the Langmuir isotherm model and Fe(III) obeys the Freundlich isotherm. Adsorption kinetics of Cr(VI) can be explained by the pseudo-second-order kinetic model while Fe(III) can be illustrated with the Lagergren-first-order model. The adsorption rate was high at lower metal ions concentration for both metal ions.

Acknowledgments

This research was funded by GPF025A-2019, Universiti Malaya Impact-Oriented Interdisciplinary Research Grant (IIRG006A-19IISS), Department of Mechanical Engineering and Department of Chemical Engineering, Faculty of Engineering, and Department of Chemistry, Faculty of Science.

References

[1] P.H. Gleick, Water in Crisis: A Guide to the World's Fresh Water Resources, Oxford University Press, Oxford, 1993.
[2] D.H. Kumar Reddy, S.M. Lee, Water pollution and treatment technologies, J. Environ. Anal. Toxicol., 2 (2012) 1–2, doi: 10.4172/2161-0525.1000e103.
[3] S.N. Sin, H. Chua, W. Lo, L.M. Ng, Assessment of heavy metal cations in sediments of Shing Mun River, Hong Kong, Environ. Int., 26 (2001) 297–301.
[4] P.D. Armitage, M.J. Bowes, H.M. Vincent, Long-term changes in macroinvertebrate communities of a heavy metal polluted

stream: the river Nent (Cumbria, UK) after 28 years, River Res. Appl., 23 (2007) 997–1015.
[5] G.L. Yuan, C. Liu, L. Chen, Z. Yang, Inputting history of heavy metals into the inland lake recorded in sediment profiles: Poyang Lake in China, J. Hazard. Mater., 185 (2011) 336–345.
[6] M.I. Fazil, S.A.B. Saleh, A.I. Mohammed, A study on heavy metal ion contamination of groundwater reserves in Beed City, Maharashtra, India, Bull. Environ. Pharmacol. Life Sci., 1 (2012) 18–21.
[7] P.B. Tchounwou, C.G. Yedjou, A.K. Patlolla, D.J. Sutton, Heavy metal toxicity and the environment, EXS, 101 (2012) 133–164.
[8] Y.K. Robert W. Peters, Evaluation of Recent Treatment Techniques for Removal of Heavy Metals from Industrial Wastewater, AIChE Symposium Series, United States, 1985.
[9] S.A. Nasreen, S. Sundarrajan, S.A. Nizar, R. Balamurugan, S. Ramakrishna, Advancement in electrospun nanofibrous membranes modification and their application in water treatment, Membranes, 3 (2013) 266–284.
[10] K. Kalantari, A.M. Afiffi, A. Salleh, E.N. Mohamad, Z. Izadiyan, Evaluation of heavy metals removal by cross-linked (polyvinyl alcohol/chitosan/magnetic) nanofibrous membrane prepared by electrospinning technique, Desal. Water Treat., 98 (2017) 266–275.
[11] F. Ebrahimi, A. Sadeghizadeh, F. Neysan, M. Heydari, Fabrication of nanofibers using sodium alginate and poly(vinyl alcohol) for the removal of $Cd^{(2+)}$ ions from aqueous solutions: adsorption mechanism, kinetics and thermodynamics, Heliyon, 5 (2019) 1–10, doi: 10.1016/j.heliyon.2019.e02941.
[12] U. Habiba, T.C. Joo, T.A. Siddique, A. Salleh, B.C. Ang, A.M. Afifi, Effect of degree of deacetylation of chitosan on adsorption capacity and reusability of chitosan/polyvinyl alcohol/TiO_2 nano composite, Int. J Biol. Macromol., 104 (2017) 1133–1142.
[13] U. Habiba, A.M. Afifi, A. Salleh, B.C. Ang, Chitosan/(polyvinyl alcohol)/zeolite electrospun composite nanofibrous membrane for adsorption of Cr^{6+}, Fe^{3+} and Ni^{2+}, J. Hazard Mater., 322 (2017) 182–194.
[14] E. Guibal, Interactions of metal ions with chitosan-based sorbents: a review, Sep. Purif. Methods, 38 (2004) 43–74.
[15] A. Cooper, R. Oldinski, H. Ma, J.D. Bryers, M. Zhang, Chitosan-based nanofibrous membranes for antibacterial filter applications, Carbohydr. Polym., 92 (2013) 254–259.
[16] S. Adibzadeh, S. Bazgir, A.A. Katbab, Fabrication and characterization of chitosan/poly(vinyl alcohol) electrospun nanofibrous membranes containing silver nanoparticles for antibacterial water filtration, Iran. Polym. J., 23 (2014) 645–654.
[17] H.F. Alharbi, M.Y. Haddad, M.O. Aijaz, A.K. Assaifan, M.R. Karim, Electrospun bilayer PAN/chitosan nanofiber membranes incorporated with metal oxide nanoparticles for heavy metal ion adsorption, Coatings, 10 (2020) 1–19, doi: 10.3390/coatings10030285.
[18] K. Huanbutta, W. Sittikijyothin, T. Sangnim, Development and characterization of bilayer wound healing patch nanofiber fabricated by electrospinning, J. Nano Res., 59 (2019) 46–56.
[19] E.S. Cozza, O. Monticelli, E. Marsano, P. Cebe, On the electrospinning of PVDF: influence of the experimental conditions on the nanofiber properties, Polym. Int., 62 (2013) 41–48.
[20] I.K. Dimzon, T.P. Knepper, Degree of deacetylation of chitosan by infrared spectroscopy and partial least squares, Int. J. Biol. Macromol., 72 (2015) 939–945.
[21] L. Li, Y.L. Hsieh, Chitosan bicomponent nanofibers and nanoporous fibers, Carbohydr. Res., 341 (2006) 374–381.
[22] H. Homayoni, S.A.H. Ravandi, M. Valizadeh, Electrospinning of chitosan nanofibers: processing optimization, Carbohydr. Polym., 77 (2009) 656–661.
[23] B. Li, F. Zhou, K. Huang, Y. Wang, S. Mei, Y. Zhou, T. Jing, Environmentally friendly chitosan/PEI-grafted magnetic gelatin for the highly effective removal of heavy metals from drinking water, Sci. Rep., 7 (2017) 1–9, doi: 10.1038/srep43082.
[24] S.P. Mishra, S.S. Dubey, D. Tiwari, Ion-exchangers in radioactive waste management Part XIV: Removal behavior of hydrous titanium oxide and sodium titanate for Cs(I), J. Radioanal. Nucl. Chem., 261 (2004) 457–463.
[25] H. Zheng, Y. Du, J. Yu, R. Huang, L. Zhang, Preparation and characterization of chitosan/poly(vinyl alcohol) blend fibers, J. Appl. Polym. Sci., 80 (2001) 2558–2565.
[26] H. Sun, L. Lu, X. Chen, Z. Jiang, Surface-modified zeolite-filled chitosan membranes for pervaporation dehydration of ethanol, Appl. Surf. Sci., 254 (2008) 5367–5374.
[27] A.A. Kittur, S.S. Kulkarni, M.I. Aralaguppi, M.Y. Karidurganavar, Preparation and characterization of novel pervaporation membranes for the separation of water–isopropanol mixtures using chitosan and NaY zeolite, J. Membr. Sci., 247 (2005) 75–86.
[28] J. Bai, Y. Li, S. Yang, J. Du, S. Wang, J. Zheng, Y. Wang, Q. Yang, X. Chen, X. Jing, A simple and effective route for the preparation of poly(vinylalcohol) (PVA) nanofibers containing gold nanoparticles by electrospinning method, Solid State Commun., 141 (2007) 292–295.
[29] Y.-T. Jia, J. Gong, X.-H. Gu, H.-Y. Kim, J. Dong, X.-Y. Shen, Fabrication and characterization of poly(vinyl alcohol)/chitosan blend nanofibers produced by electrospinning method, Carbohydr. Polym., 67 (2007) 403–409.
[30] H. Bai, X. Wang, Y. Zhou, L. Zhang, Preparation and characterization of poly(vinylidene fluoride) composite membranes blended with nano-crystalline cellulose, Prog. Nat. Sci., 22 (2012) 250–257.
[31] D.P. Subedi, Contact angle measurement for the surface characterization of solids, Himalayan Phys., 11 (2011) 1–4, doi: 10.3126/hj.v2i2.5201.
[32] T. Yeamsuksawat, J. Liang, Characterization and release kinetic of crosslinked chitosan film incorporated with α-tocopherol, Food Packag. Shelf Life, 22 (2019) 1–9, doi: 10.1016/j.fpsl.2019.100415.
[33] M.N.V.R. Kumar, A review of chitin and chitosan applications, React. Funct. Polym., 46 (2000) 1–27.
[34] A. Çay, M. Miraftab, E.P.A. Kumbasar, Characterization and swelling performance of physically stabilized electrospun poly(vinyl alcohol)/chitosan nanofibres, Eur. Polym. J., 61 (2014) 253–262.
[35] M. Li, S. Cheng, H. Yan, Preparation of crosslinked chitosan/poly(vinyl alcohol) blend beads with high mechanical strength, Green Chem., 9 (2007) 1–5.
[36] A.M. Zaharia, A.R.M. Yusoff, N.A. Buang, P. Satishkumar, M.J.F. Jasni, Z. Yusop, Fabrication and characterization of polyvinylidene fluoride composite nanofiber membrane for water flux property, J. Teknol., 74 (2015) 9–14.
[37] J. Pu, K. Komvopoulos, Mechanical properties of electrospun bilayer fibrous membranes as potential scaffolds for tissue engineering, Acta Biomater., 10 (2014) 2718–2726.
[38] J.H. Park, B.S. Kim, Y.C. Yoo, M.S. Khil, H.Y. Kim, Enhanced mechanical properties of multilayer nano-coated electrospun nylon 6 fibers via a layer-by-layer self-assembly, J. Appl. Polym. Sci., 107 (2008) 2211–2216.
[39] S. Ahmady-Asbchin, Y. Andres, C. Gerente, P.L. Cloirec, Biosorption of Cu(II) from aqueous solution by *Fucus serratus*: surface characterization and sorption mechanisms, Bioresour. Technol., 99 (2008) 6150–6155.
[40] S. Deng, Y.P. Ting, Polyethylenimine-modified fungal biomass as a high-capacity biosorbent for Cr(VI) anions: sorption capacity and uptake mechanisms, Environ. Sci Technol., 39 (2005) 8490–8496.
[41] Y.S. Ho, G. Mckay, Pseudo-second order model for sorption processes, Process Biochem., 34 (1999) 451–465.
[42] X. Chen, Modeling of experimental adsorption isotherm data, Information, 6 (2015) 14–22.
[43] X. Song, Y. Zhang, C. Yan, W. Jiang, C. Chang, The Langmuir monolayer adsorption model of organic matter into effective pores in activated carbon, J. Colloid Interface Sci., 389 (2013) 213–219.
[44] V. Vimonses, S. Lei, B. Jin, C.W.K. Chow, C. Saint, Kinetic study and equilibrium isotherm analysis of Congo Red adsorption by clay materials, Chem. Eng., 148 (2009) 354–364.
[45] E. Ajenifuja, J.A. Ajao, E.O.B. Ajayi, Adsorption isotherm studies of Cu(II) and Co(II) in high concentration aqueous solutions on photocatalytically modified diatomaceous ceramic adsorbents, Appl. Water Sci., 7 (2017) 3793–3801.
[46] S. Chatterjee, S. Chatterjee, B.P. Chatterjee, A.K. Guha, Adsorptive removal of Congo red, a carcinogenic textile dye by chitosan hydrobeads: binding mechanism, equilibrium and kinetics, Colloids Surf., A, 299 (2007) 146–152.